

This article was downloaded by:

On: 25 January 2011

Access details: Access Details: Free Access

Publisher Taylor & Francis

Informa Ltd Registered in England and Wales Registered Number: 1072954 Registered office: Mortimer House, 37-41 Mortimer Street, London W1T 3JH, UK



## Separation Science and Technology

Publication details, including instructions for authors and subscription information:

<http://www.informaworld.com/smpp/title~content=t713708471>

### Membrane Reactor/Separator: A Design for Bimolecular Reactant Addition

A. L. Y. Tonkovich<sup>a</sup>; R. B. Secker<sup>a</sup>; E. L. Reed<sup>a</sup>; G. L. Roberts<sup>a</sup>; J. L. Cox<sup>a</sup>

<sup>a</sup> Chemical Technology Department, Pacific Northwest Laboratory, Richland, WA

**To cite this Article** Tonkovich, A. L. Y. , Secker, R. B. , Reed, E. L. , Roberts, G. L. and Cox, J. L.(1995) 'Membrane Reactor/Separator: A Design for Bimolecular Reactant Addition', Separation Science and Technology, 30: 7, 1609 — 1624

**To link to this Article:** DOI: 10.1080/01496399508010365

URL: <http://dx.doi.org/10.1080/01496399508010365>

## PLEASE SCROLL DOWN FOR ARTICLE

Full terms and conditions of use: <http://www.informaworld.com/terms-and-conditions-of-access.pdf>

This article may be used for research, teaching and private study purposes. Any substantial or systematic reproduction, re-distribution, re-selling, loan or sub-licensing, systematic supply or distribution in any form to anyone is expressly forbidden.

The publisher does not give any warranty express or implied or make any representation that the contents will be complete or accurate or up to date. The accuracy of any instructions, formulae and drug doses should be independently verified with primary sources. The publisher shall not be liable for any loss, actions, claims, proceedings, demand or costs or damages whatsoever or howsoever caused arising directly or indirectly in connection with or arising out of the use of this material.

MEMBRANE REACTOR/SEPARATOR: A DESIGN FOR  
BIMOLECULAR REACTANT ADDITION

A. L. Y. Tonkovich , R. B. Secker, E. L. Reed, G. L. Roberts, J. L. Cox  
Chemical Technology Department  
Pacific Northwest Laboratory  
Battelle Boulevard  
Richland, WA 99352

ABSTRACT

A membrane reactor (MBR) is used to investigate the effect of selective reactant addition on series-parallel reaction networks, such as the oxidative dehydrogenation of ethane to ethylene. Ethylene is favored in an oxygen-lean environment, while excess oxygen favors the formation of combustion products. Control of the reactant ratio (ethane to oxygen) is crucial to both the overall selectivity and the hydrocarbon conversion. Traditional reactor designs co-feed the bimolecular reactants at the top of the reactor at some preset feed ratio. The MBR uses a tube (porous alumina membrane) and shell configuration. One reactant is fed at the top of a catalyst bed packed within the membrane core. The other reactant permeates into the tube along the length of the reactor via an imposed pressure drop. The reactant ratio is large at the top of the MBR, which leads to high selectivities; as the oxygen is consumed, it is replenished via downstream permeation to improve the ethane conversion. The MBR and a plug flow reactor (PFR) are evaluated at 600 °C, with identical space velocities, and using a magnesium oxide catalyst doped with samarium oxide. At low to moderate reactant feed ratios, the ethylene yield in the MBR exceeds the PFR by a factor of three, under some conditions. At higher feed ratios, the performance of the PFR nears or exceeds the performance of the MBR.

## INTRODUCTION

Membrane reactors are under investigation as an energy efficient and environmentally benign alternative to traditional reactor designs. Many of the reactions of interest to the chemical and petrochemical industries involve high-temperature, gas-phase, solid-catalyzed processes. Inorganic membrane reactors can withstand the elevated process temperatures, and have the potential to improve product yields per pass for some of these reactions. Yield improvements reduce the formation of undesired side products which require disposal, thus preventing pollution. Higher yields per pass also reduce the separation and recycle load of the unreacted material, and therefore lower process energy requirements.

Several types of inorganic membrane reactors exist. The most common type continuously separates products from reactants to drive otherwise equilibrium-limited reactions towards completion. Dehydrogenation reactions represent a potential application, where hydrogen is selectively removed from alkane/alkene mixtures.

The membrane reactor (MBR) described in this paper selectively permeates one reactant along the length of the reactor to control local reactant ratios. This design has applications for series-parallel reaction networks, such as partial oxidation reactions. The bi-molecular reactant ratio determines which reaction pathway is favored, and the control of this ratio in the MBR allows for increased product yields. The oxidative dehydrogenation of ethane to ethylene is evaluated in a MBR. The performance of the MBR is compared with the performance of the standard industrial reactor, the plug flow reactor (PFR).

## BACKGROUND

The most common application for inorganic membrane reactors has been the *in situ* separation of hydrogen during dehydrogenation reactions to improve product yields which are limited by equilibrium constraints (1-10).

Other MBR configurations have been presented. One design feeds reactants from either side of a membrane to react in catalytically impregnated membrane

pores (11-17). Another MBR design selectively adds oxygen to a reaction zone via transport across a dense membrane made of materials such as zirconia, silver, and the like. These permselective materials transport molecular oxygen (18-26).

A theoretical configuration has also been presented for partial oxidation reactions; the intermediate product is separated from the reactants by the use of a permselective inorganic membrane (27-29).

### EXPERIMENTAL

A MBR is constructed in a tube and shell configuration to evaluate the effect of reactor design (a continuous air feed along the axis of the reactor rather than an air feed at the top of the reactor) on partial oxidation reactions. A porous rather than a dense membrane is used in this study to feed air to a reaction zone. An imposed trans-membrane pressure drop prevents back permeation.

#### Reaction Network

The oxidative dehydrogenation of ethane to ethylene is investigated (equations 1-3). This partial oxidation reaction is coupled with the competing series-parallel combustion reactions, and occurs catalytically.



The Delplot method (30) is used to verify the series-parallel nature of this reaction network. Ethylene is the only primary product. Carbon dioxide and carbon monoxide are determined to be secondary products from the Delplot method, and thus they are formed from ethylene. Trace amounts of methane are produced in some experiments. There is insufficient data to conclude from this method if methane is a primary or higher-ordered product. At the reaction temperature (600 °C), pyrolysis is not observed.

### Catalyst

This reaction network is studied using a magnesium oxide catalyst doped with lithium nitrate, ammonium chloride, and samarium oxide. The preparation procedure is slightly varied from another published source (31). The only variation is the substitution of samarium oxide for the other lanthanide series dopants. The pre-calcined solid mixture is made of 58.1 wt% MgO, 24.3% LiNO<sub>3</sub>, 13.8% NH<sub>4</sub>Cl, and 3.82% Sm<sub>2</sub>O<sub>3</sub>. All chemicals are obtained from Aldrich Chemicals in high-purity form. X-ray diffraction (XRD) experiments show that the calcined catalyst has lost most of the ammonium and nitrates, and has formed a multi-phase system.

The microreactor experiments are run with a 70-100 mesh catalyst powder, which gives a pressure drop of 8 psi. The MBR and PFR experiments use larger catalyst particles (25-40 or 40-70 mesh) to reduce the operating pressures.

### Membrane Reactor Configuration

The MBR employs a tube and shell configuration to independently feed bi-molecular reactants. One reactant is fed shell side and permeates through an inorganic membrane into the reaction zone. The other reactant is fed at the top of the catalyst packed tube (porous alumina membrane). This configuration is presented in Figure 1.

Two types of membranes are used in this study. The first is a Membralox® membrane from US Filter (Warrendale, PA). The tube is composed of a graded pore structure of mostly  $\alpha$ -alumina; the outer layers consist of 12- $\mu$ m pores, followed by 0.8- $\mu$ m and 0.2- $\mu$ m pores; each layer has a thickness of 1.5 mm, 40  $\mu$ m, and 20  $\mu$ m, respectively. The innermost layer is made of  $\gamma$ -alumina and has a mean pore diameter of 50  $\text{\AA}$ . This "skin" is approximately 4  $\mu$ m thick. The overall wall thickness is 1.5 mm. The tube has an internal diameter of approximately 7 mm and an outer diameter of 10 mm. A length of 20.8 cm is packed with the catalyst in the membrane reactor.

The second membrane evaluated is a porous  $\alpha$ -alumina tube from Coors (Golden, CO). The mean pore diameter through the entire width of the tube is 200  $\text{\AA}$ . The tubes have an internal diameter of 7 mm and outer diameter of 10 mm. The tube is 7 cm long, of which 4 cm are packed with catalyst.

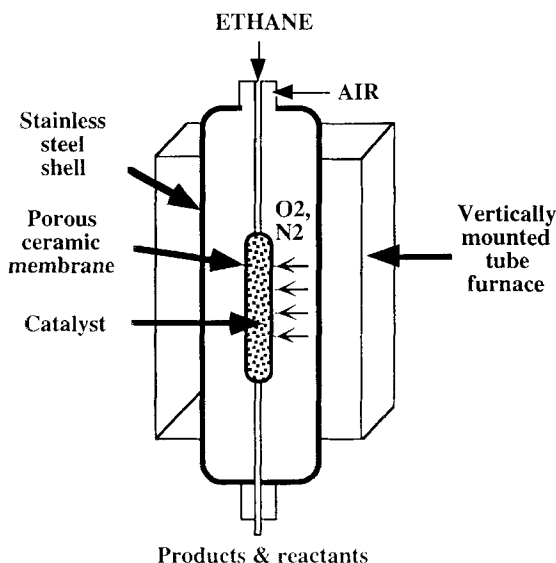


Figure 1. Tube and shell membrane reactor configuration.

Each membrane is placed in the center of a stainless steel shell. A gas-tight, high-temperature ( $T=600\text{ }^{\circ}\text{C}$ ) seal in an oxidizing environment is maintained between the membrane and the shell; this is a non-trivial problem. The Membralox membranes have a factory-coated glaze on both ends of the tube and are readily sealed with stainless steel Swagelock nuts and graphite ferrules. The Coors tubes, however, have porous ends and require a graded seal to maintain a hermetic junction, see Figure 2. The graded seal consists of joining a glazed porous membrane to a dense ceramic tube with the aid of a ceramic cement.

A glaze (Aremco-seal 617, from Aremco Products, Inc., Ossing, NY) is coated to approximately 1 cm of each end of the porous membrane to continuously seal both the outer and inner membrane surface. The length of the sealed ends is not included in the length of the reactor. It is vital to glaze the membrane ends to prevent the reactant gases from channeling around the ends of the tube. Stainless steel nuts with graphite ferrules (made of preformed graphite ferrules, graphite string, graphite ribbon, or graphite packing material) placed around the end of an

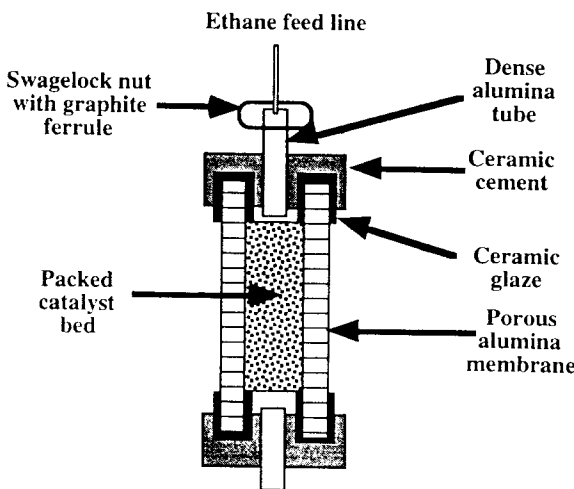


Figure 2. Graded-seal used to maintain gas-tight seal between porous membrane and feed line.

uncoated porous substrate does not maintain a gas-tight seal at 600 °C in all cases. The graphite ferrules do not leak when sealed to a smooth (non-porous) surface.

A dense alumina tube (6.5-mm OD and 3-mm ID) is partially inserted inside the porous membrane and joined to the Aremco glaze with a ceramic cement, Autostick (Carlton Brown and Partners LTD, Sheffield, England). The cement maintains a high-temperature, gas-tight seal between the glaze-coated porous membrane and the non-porous alumina tube. The cement will not maintain a gas-tight seal with the porous material. Stainless steel nuts and graphite ferrules join 1/8-in. stainless steel gas lines to the dense alumina tube inserts.

Temperature cycling cracks the cement; this is avoided by maintaining a minimum temperature of 400 °C with a nitrogen purge when not in use.

The outer shell is made of a 2.54-cm OD, Schedule 40 stainless steel tube and is 54.61 cm in length. Two grooved end caps are used to maintain a gas-tight seal between the shell and the environment. The entire shell is placed inside a vertically mounted tube furnace. The ends of the shell do not sit in the furnace, and thus do not require the same rigorous materials choice to maintain a gas-tight seal at the elevated temperatures. The grooved end caps screw into grooves in the shell and are sealed with graphite gaskets. A wide-bore Swagelock fitting is

welded on each endcap to permit the 1/8-in. stainless steel feed tubes connected to the membrane to enter and exit the shell. The stainless steel tubes exiting the endcaps are sealed using compression fittings and vespel ferrules.

The shell with the internal tube is vertically mounted in a Keith two-zone furnace, which is 45.72 cm in length. A Eurotherm controller on the furnace maintains the temperature in each zone to within 1 °C of the target 600 °C. Additional thermocouples are mounted inside the furnace and on the reactor shell. Experimental difficulties did not allow thermocouples to be placed inside the MBR to measure the *in situ* temperature or temperature rises during the reaction.

The catalyst reaction zone varies from 20.8 cm to 4 cm for the two sets of experiments. A heated dead-space sits above this zone to pre-heat the reactants.

Pressure gauges are mounted to the shell, at the top of the tube (membrane), and at the reactor outlet. This allows for accurate measurements of the trans-membrane pressure drop and the axial pressure drop across the catalyst bed. The trans-membrane pressure drop is proportional to the permeation or mass flux of air across the membrane. The other reactant (ethane) is fed to the tube with an Aalborg AFC 2600 series mass flow controller.

#### Plug Flow Reactor Configuration

The MBR is compared with the performance of a PFR, which is constructed with a dense alumina tube of similar dimensions (6.5-mm ID) to the membrane. The PFR is packed with the same catalyst sample used in the MBR experiments.

The ends of the tube are placed outside the hot zone of the Keith vertically mounted tube furnace. Graphite ferrules in Swagelock fittings are used to seal the ends of the tube.

The packed catalyst bed is placed in the center of the tube furnace to maintain a uniform temperature profile and to allow the reactants ample time to pre-heat to the reaction temperature.

The bimolecular reactants are added with the Aalborg mass flow controllers and mixed in a tee before being co-fed at the top of the reactor.

#### Gas Analysis

The products in each reactor are analyzed via gas chromatography. A Carle Hach gas chromatograph with three columns connected in series (1.83-m column

packed with 50-80 mesh 80% Porapak N and 20% Porapak Q, 2.13-m column packed with 80-100 mesh Molecular Sieve 13X, and a .91-m column packed with 80-100 mesh Molecular Sieve 5A) is used to analyze the light gases (ethane, ethylene, carbon dioxide, carbon monoxide, methane, nitrogen, and oxygen). A helium carrier is used with a flowrate of 28 cm<sup>3</sup>/min, and the oven temperature is set at 65 °C. The reported areas are converted to mole fractions via independent calibrations for each gas. The calibrations are checked at least once per month to detect a base-line shift from water sorption. The columns are re-conditioned as needed.

### Calculations

The ethane conversion, ethylene selectivity, ethylene yield, and oxygen conversion are calculated from the calibrated GC mole percents (n<sub>i</sub>). The ethylene yield is taken as the conversion of ethane multiplied by the ethylene selectivity. The denominator in the oxygen conversion calculation represents the initial moles of oxygen, where Ratio denotes the inlet ethane to oxygen feed ratio. The numerator in the oxygen conversion equation represents the moles of oxygen converted from the three overall reaction steps (.5 moles of oxygen are required to produce one mole of ethylene, 2.5 moles of oxygen produce 2 moles of CO, and 3.5 moles of oxygen produce two moles of CO<sub>2</sub>).

$$C_{\text{ethane}} = \frac{n_{\text{ethylene}} + .5(n_{\text{CO}_2} + n_{\text{CO}} + n_{\text{CH}_4})}{n_{\text{ethane}} + n_{\text{ethylene}} + .5(n_{\text{CO}_2} + n_{\text{CO}} + n_{\text{CH}_4})} \quad (4)$$

$$S_{\text{ethylene}} = \frac{n_{\text{ethylene}}}{n_{\text{ethylene}} + .5(n_{\text{CO}_2} + n_{\text{CO}} + n_{\text{CH}_4})} \quad (5)$$

$$C_{\text{O}_2} = \frac{.5n_{\text{C}_2\text{H}_4} + 1.25n_{\text{CO}} + 1.75n_{\text{CO}_2}}{(.5n_{\text{CO}_2} + .5n_{\text{CO}} + n_{\text{C}_2\text{H}_4} + n_{\text{C}_2\text{H}_6} + .5n_{\text{CH}_4}) / \text{Ratio}} \quad (6)$$

### RESULTS AND DISCUSSION

After the catalyst is prepared, it is ground and sieved to 70-100 mesh and evaluated in a quartz microreactor. Figure 3 plots the ethane conversion and

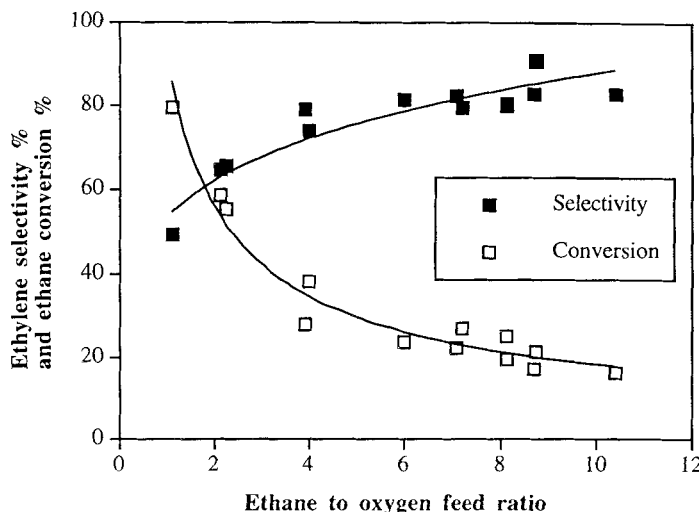


Figure 3. Catalyst microreactor results at  $T=600\text{ }^{\circ}\text{C}$  and space velocity =  $7.9\text{ cm}^3/\text{min}\cdot\text{gcat}$ .

ethylene selectivity as a function of feed ratio at a fixed space velocity of  $7.9\text{ cm}^3/\text{min}\cdot\text{gcat}$  and  $600\text{ }^{\circ}\text{C}$ ; this corresponds to a residence time of approximately 5 seconds. Increasing ethylene selectivity and decreasing ethane conversion are observed as the reactant feed ratio (ethane to oxygen) increases. Complete oxygen conversion is observed at the higher feed ratios. A pressure drop of 8 psi is observed during the microreactor trials. Larger catalyst particles (25-40 mesh or 40-70 mesh) are used in the MBR and corresponding PFR experiments to lower the axial pressure drop.

The first set of MBR experiments uses a Membralox 50 Å membrane. Figure 4 plots the ethylene product yield as a function of the inlet reactant feed ratio for residence times of 3.9, 5.5, and 8.7 seconds, which corresponds to space velocities of 102.5, 72.5, and  $45.8\text{ cm}^3/\text{min}\cdot\text{gcat}$ , respectively. The residence time is defined as the reactor volume divided by the sum of the feed flowrates. The membrane is packed with 1.2 g of 25-40 mesh catalyst, which has been mixed with 25-40 mesh catalytically inert alumina chips.

In these trials at  $600\text{ }^{\circ}\text{C}$ , the MBR shows enhanced ethylene yields (5% to 10% higher) at lower feed ratios (less than 1). At the higher feed ratios, there is

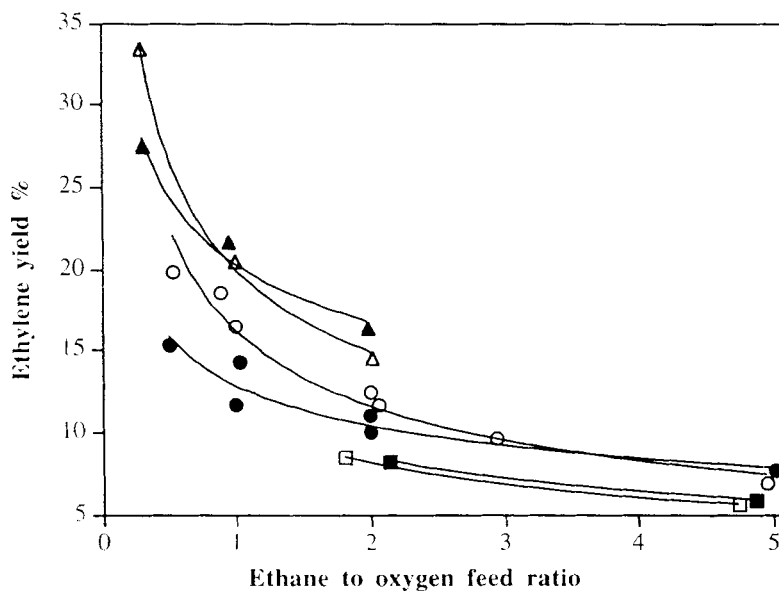


Figure 4. Ethylene yield for MBR and PFR trials using a Membralox<sup>®</sup> 50 Å membrane at  $T=600^{\circ}\text{C}$ ; residence times of 3.9 (-□-), 5.5 (-○-), and 8.7 (-△-) seconds. Closed symbols -- PFR, open symbols -- MBR.

little observable difference between the reactor yields. The ethane and oxygen conversion in the MBR exceeds the conversions obtained with the PFR by 10% to 25%. The selectivity in the MBR is lower than in the PFR by approximately 10% to 15%. It is believed that catalytic wall effects are playing a role in the deterioration of the ethylene selectivity.

The pressure drop across the Membralox tube ranges between 10 and 50 psi, and no back permeation is observed. This, however, is not true for the other Membralox tubes. The tube used in these trials was later tested at room temperature in a water bath to observe the uniformity of permeation. Most of the pores were fused, and permeation only occurred along a narrow axial line down the tube. Experimental membrane pre-heat treatments may have altered this tube. The other Membralox tubes do not maintain similarly high pressure drops with the same air flowrates; their average pressure drop ranges between 0.2 and 1 psi.

Back permeation of reactants and products from the tube to the shell is a significant problem in this pressure drop range.

The reported results do not reflect the true performance of a MBR; while the feed is equally split along the length of the reactor, it is not equally split at all angular points around the membrane. This imposes concentration gradients in all three cylindrical directions, which may impact the reactor performance in the limit of slow radial and angular mass transfer.

For this MBR application, it is desirable to have the selective layer of the inorganic membrane be thicker than that commercially available with the Membralox tubes to maintain a sufficient trans-membrane pressure drop. These membranes should work well for liquid-phase reaction applications, where they readily maintain a high trans-membrane pressure drop.

The second set of MBR experiments uses a Coors 200 Å porous  $\alpha$ -alumina membrane. This membrane has a wall thickness of 1.5 mm, which increases the resistance to flow. A 4-cm reactor length is used to lower the overall surface area and thus enable the desired trans-membrane pressure drop. The pressure drop across an unmodified membrane ranges between 1 and 5 psi, depending on the air flowrate; at these pressure drops, back permeation of the products and reactants occurs. The tube is internally coated to reduce the available surface area. Two equidistant 1-mm axial strips are left open, while the remaining 80% of the internal surface area is coated with the 617-Aremco glaze. The glaze was tested and found to be inert at the reaction conditions.

Back permeation experiments are done at 600 °C with the modified Coors membranes to determine the operating pressure range that prevents the ethane and products from entering the membrane pores and possibly the outer shell. The air flowrate across the membrane is set to achieve a preset trans-membrane pressure drop, and then the ethane flow is sent to the reaction tube at time  $t=0$ . Ethane breakthrough curves for different trans-membrane pressure drops are measured as a function of time (between 5 seconds and 5 minutes). The ethane flow is set between 25% and 35% of the total.

If there is no back permeation, then no "dispersive-like" force is introduced to the ethane flow, and it should uniformly move through the reactor and exit at some time (equal to the residence time) later. If there is back permeation, the exiting ethane concentration will gradually increase as a function of time. Figure 5 shows a series of breakthrough curves obtained with the modified Coors tube.

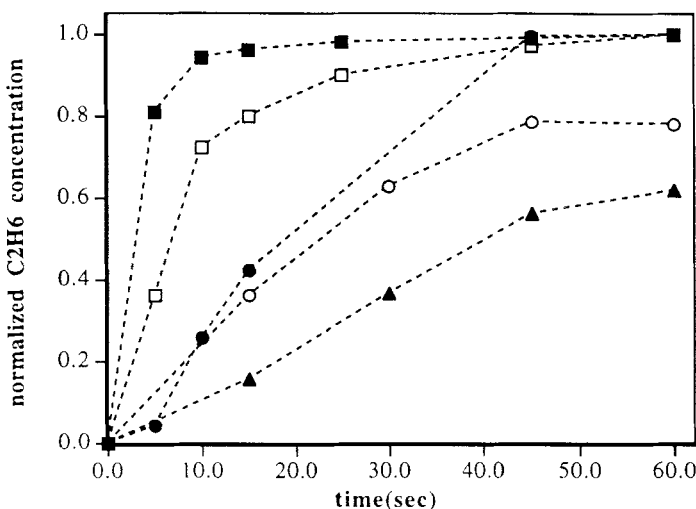


Figure 5. Effect of trans-membrane pressure drop on back permeation of reactants and products; normalized ethane concentration vs. time for 10.5 (- ■ -), 8.5 (- □ -), 6 (- ● -), 4.0 (- ○ -), and 2.0 (- ▲ -) psig.

For this type and length of membrane, a trans-membrane pressure drop of at least 6 to 7 psi is required to keep all reactants and products within the membrane core. At the lower pressure drops, trans-membrane flow of ethane is observed. The ethane is converted to carbon dioxide on the shell side, which later exits the system.

MBR experiments at 600 °C using the modified Coors membranes show a dramatic increase in the ethylene yield, see Figure 6. Residence times of 1.6 and 2.25 seconds are used, which correspond to space velocities of 39 and 27  $\text{cm}^3/\text{min}\cdot\text{gcat}$ , respectively. For these trials, the trans-membrane pressure drop ranges between 5 and 20 psi. The membrane is packed with 1.5 g of 40-70 mesh catalyst. The largest improvement in ethylene yield is observed at the lowest feed ratio. At a residence time of 1.6 seconds and a feed ratio of .3, the ethylene yield is 11% in the PFR and 34% in the MBR. At the longer residence time of 2.25 seconds and a feed ratio of .3, the MBR still outperforms the PFR but with a lower magnitude. The ethylene yield in the MBR is 32%, and 14% in the PFR. As the feed ratio increases, the reactor yields approach each other.

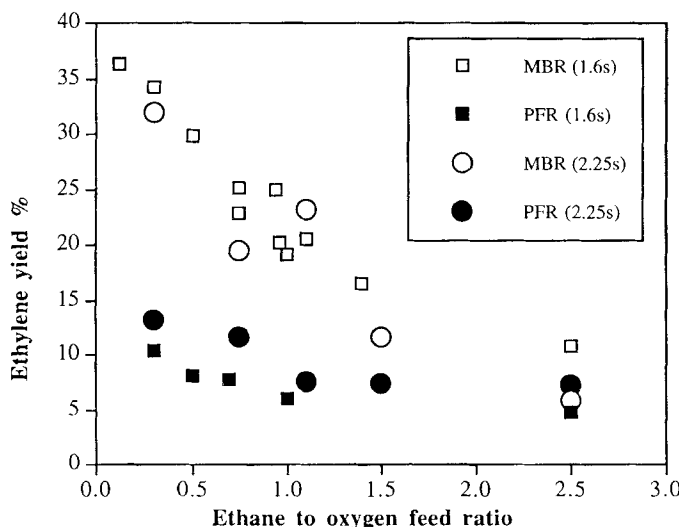


Figure 6. Ethylene yield for MBR and PFR trials using a Coors 200 Å membrane at  $T=600$  °C; residence times of 1.6 (-□-) and 2.25 (-○-) seconds. Closed symbols -- PFR, open symbols -- MBR.

This behavior is the result of two phenomena. At the high ratios, the desired product selectivity is high and further splitting of the feed produces incremental improvements. At low ratios, the desired product selectivity is low, and splitting the feed has a large impact.

The other phenomenon is an alteration in the residence time distribution. At low feed ratios, a large amount of air permeates through the membrane and a small amount of ethane is added. The ethane superficial velocity increases as downstream permeation occurs, therefore long contact times with favorable feed ratios occur at the top of the column. As the hydrocarbon moves down the column, its ratio with oxygen becomes less favorable; but the catalyst contact time decreases, which favors the intermediate product. The MBR thus outperforms the PFR at low feed ratios.

At high feed ratios, a smaller relative amount of air is fed to the reactor, and thus the ethane catalyst contact time only varies slightly down the reactor. In addition, little added benefit is derived from increasing an already high feed ratio, thus the performance of the MBR and PFR approach each other.

### CONCLUSIONS

The MBR employs a tube and shell configuration to selectively add one bimolecular reactant to the other. The ratio of these reactants determines the favored reaction pathway in a series-parallel reaction network, such as the oxidative dehydrogenation of ethane. The oxygen feed is equally split axially along the length of the reactor. The local reactant ratio at the top of the reactor is high and thus favors the production of ethylene. Downstream permeation replenishes the consumed oxygen to improve the conversion of ethane.

Improved ethylene yields are observed with the MBR at low to moderate inlet feed ratios. The performance of the MBR approaches the PFR at higher feed ratios. The ethylene yields, at the lower feed ratios, have shown a three-fold increase in the MBR over the PFR. These results are preliminary, and optimization of the MBR parameters may give higher yield improvements.

While the development of this inorganic MBR configuration presents potential advantages for some reaction pathways (series-parallel, or parallel reactions of different orders), additional characterization is required.

### ACKNOWLEDGMENTS

This research was supported by the U.S. Department of Energy (DOE) under the Energy Technology Development Initiative, a Laboratory Directed Research and Development program at Pacific Northwest Laboratory.

Pacific Northwest Laboratory is operated for DOE by Battelle Memorial Institute under Contract DE-AC06-76RLO 1830.

Mr. Secker and Mr. Reed gratefully acknowledge support from the DOE, Division of University and Industry Programs, Office of Energy Research, as Science and Engineering Research Semester program participants at Pacific Northwest Laboratory.

### REFERENCES

1. Hsieh, H., AICHE Symposium series 268, 85, 53 (1989).
2. Hsieh, H., Catal. Rev.-Sci. Eng., 33(1&2), 1 (1991).

3. Ilias, S., Govind, R., *AICHE Symposium Series* 268, 85, 18 (1989).
4. Noble, R., *Div. Pet. Chem ACS*, 37(1), 11 (1992).
5. Falconer, J., Noble, R., Sperry, D., in Membrane Separations Technology: Principles and Applications, S. Stern and R. Noble, Eds., Elsevier Science Publishers, 1993.
6. Shu, J., Grandjean, B., Van Neste, A., Kaliaguine, S., *Can. J. Chem. Eng.*, 69, 1036 (1991).
7. Gryaznov, M., *Plat. Met. Rev.*, 36(2), 70 (1992).
8. Tsotsis, T., Champagnie, A., Vasileiadis, S., Ziaka, Z., Minet, R., *Sep. Sci. Technol.*, 28(1-3), 397 (1993).
9. Keizer, K., Zaspalis, V., Burggraaf, T., in Ceramics Today -Tomorrow's Ceramics, P. Vincenzini, Ed., Elsevier Science Publishers, 1991, p. 2511.
10. Armor, J., *Appl. Cat.*, 49(1), 1 (1989).
11. Sloot, H., Versteeg, G., van Swaaij, W., *Chem. Eng. Sci.*, 45(8), 2415 (1990).
12. Sloot, H., Versteeg, G., Smolders, C., van Swaaij, W., *Key Eng. Mat.*, 61&62, 261 (1991).
13. Veldsink, J., van Damme, R., Versteeg, G., van Swaaij, W., *Chem. Eng. Sci.*, 47(9-11), 2939 (1992).
14. Zaspalis, V., van Praag, W., van Ommen, J., Ross, J., Burggraaf, A., *Appl. Cat.*, 74, 235 (1991a).
15. Zaspalis, V., Keizer, K., Ross, J., Burggraaf, A., *Key Eng. Mat.*, 61&62, 359 (1991b).
16. Zaspalis, V., van Praag, W., Keizer, K., van Ommen, J., Ross, J., Burggraaf, A., *Appl. Cat.*, 74, 205 (1991c).
17. Zaspalis, V., van Praag, W., Keizer, K., van Ommen, J., Ross, J., Burggraaf, A., *Appl. Cat.*, 74, 249 (1991d).
18. Cales, B., Baumard, J., *High Temp.-High Pres.*, 14, 681 (1982).
19. Eng, D., Stoukides, M., *Catal. Rev.-Sci. Eng.*, 33(3&4), 375 (1991).
20. Nigara, Y., Cales, B., *Bull. Chem. Soc. Jpn.*, 59, 1997 (1986).
21. Nozaki, T., Yamazaki, O., Omata, K., Fujimoto, K., *Chem. Eng. Sci.*, 47(9-11), 2945 (1992).
22. Itoh, N., Sanchez, M., Xu, W., Haraya, K., Hongo, M., *J. Mem. Sci.*, 77, 245 (1993).

23. Gryaznov, V., Vedernikov, V., Gul'yanova, S., *Kin. Kat.*, 27(1), 129 (1986).
24. Omata, K., Hashimoto, S., Tominaga, H., Fujimoto, K., *Appl. Cat.*, 52, L1 (1989).
25. Stoukides, M., Vayenas, C., *J. Cat.*, 70, 137 (1981).
26. Fujimoto, K., Asami, K., Omata, K., Hashimoto, S., in Natural Gas Conversion, Holmen, A., Ed., Elsevier Science Publishers, Amsterdam, 1991, p. 525.
27. Lund, C., *Cat. Lett.*, 12, 395 (1992).
28. Agarwalla S., Lund, C., *J. Mem. Sci.*, 70, 129 (1992).
29. Bernstein, L., Lund, C., *J. Mem. Sci.*, 77, 155 (1993).
30. Bhore, N., Klein, M., Bischoff, K., *I&EC Res.*, 29, 313 (1990).
31. Conway, S., Wang, D., Lunsford, J., *Appl. Cat. A: Gen.*, 79, L1 (1991).